# Chronic hypoxia in ovine pregnancy recapitulates physiological and molecular markers of preeclampsia in the mother, placenta and offspring

Wen Tong[1,2], Beth J. Allison[1], Kirsty L. Brain[1], Olga V. Patey[1], Youguo Niu[1-4], Kimberley J. Botting[1-3], Sage G. Ford[1], Tess A. Garrud[1,2], Peter F. B. Wooding[1,2], Caroline J. Shaw[5], Qiang Lyu[4], Lin Zhang[4], Jin Ma[4], Tereza Cindrova-Davies[1,2], Hong Wa Yung[1,2], Graham J. Burton[1,2], Dino A. Giussani*[1-4]

[1]*Department of Physiology Development & Neuroscience, University of Cambridge, United Kingdom;*

[2]*Centre for Trophoblast Research, University of Cambridge, United Kingdom*;

[3]*BHF Cardiovascular Centre for Research Excellence, University of Cambridge, United Kingdom*

[4]*Department of Aerospace Physiology, Fourth Military Medical University, Xi'an, China;*

[5]*Department of Metabolism, Digestion and Reproduction, Imperial College London, United Kingdom*

**Short Title**: Pre-eclampsia link to gestational hypoxia

**Word Counts:** Manuscript: 5,451; Abstract: 225

Figures: 6

**Corresponding Author**: Professor Dino A. Giussani PhD ScD FRCOG

Department of Physiology, Development and Neuroscience

University of Cambridge

Email: dag26@cam.ac.uk

Tel: +44(0)1223 333894

**Abstract**

**Background:** Preeclampsia continues to be a prevalent pregnancy complication and underlying mechanisms remain controversial. A common feature of preeclampsia is utero-placenta hypoxia. In contrast to the impact of hypoxia on the placenta and fetus, comparatively little is known on the maternal physiology.

**Methods:** We adopted an integrative approach to investigate the inter-relationship between chronic hypoxia during pregnancy with maternal, placental and fetal outcomes, common in preeclampsia. We exploited a novel technique using isobaric hypoxic chambers and *in vivo* continuous cardiovascular recording technology for measurement of blood pressure in sheep and studied the placental stress in response to hypoxia at cellular and sub-cellular levels.

**Results:** Chronic hypoxia in ovine pregnancy promoted fetal growth restriction with evidence of fetal brain-sparing, increased placental hypoxia-mediated oxidative damage and activated placental stress response pathways. These changes were linked with dilation of the placental endoplasmic reticulum cisternae and increased placental expression of the antiangiogenic factors sFlt-1 and sEng, combined with a shift towards an angiogenic imbalance in the maternal circulation. Chronic hypoxia further led to an increase in uteroplacental vascular resistance, and the fall in maternal blood pressure with advancing gestation measured in normoxic pregnancy did not occur in hypoxic pregnancy.

**Conclusions:** Therefore, we show in an ovine model of sea level adverse pregnancy that chronic hypoxia recapitulates physiological and molecular features of preeclampsia in the mother, placenta and offspring.

**Keywords:** chronic hypoxia, fetal growth restriction, unfolded protein response, placental dysfunction, angiogenic imbalance, oxidative stress

## Non-standard abbreviations & acronyms

| | | | |
|---|---|---|---|
| **ATF6** | activating transcription factor 6 | **$P_aO_2$** | arterial partial pressure of oxygen |
| **dGA** | days gestational age | **PDI** | protein disulfide isomerase |
| **ER** | endoplasmic reticulum | **PI** | pulsatility index |
| **ERK** | extracellular signal-regulated kinase | **PlGF** | placental growth factor |
| **FGR** | fetal growth restriction | **sEng** | soluble endoglin |
| **GRP78** | glucose-related protein 78 | **sFlt-1** | soluble fms-like tyrosine kinase 1 |
| **HIF1α** | hypoxia-inducible factor 1α | **UPR** | unfolded protein response |
| **HSP27** | heat shock protein 27 | **$UPR^{Cyt}$** | cytosolic unfolded protein response |
| **HSP70** | heat shock protein 70 | **$UPR^{ER}$** | endoplasmic reticulum unfolded protein response |
| **JNK** | C-Jun N-terminal kinase | **VEGF** | vascular endothelial growth factor |

## Background

Preeclampsia remains a leading cause of perinatal morbidity and mortality, affecting 2-8% of pregnancies worldwide[1]. Therefore, there is ongoing interest in improving our understanding of the disease. Historically, preeclampsia was thought to develop exclusively in early pregnancy due to failure of spiral artery conversion and reduced uteroplacental perfusion[2]. However, knowledge has expanded and it is now accepted that preeclampsia encompasses a broader spectrum of disorders, including early- and late-onset preeclampsia[3].

Irrespective of aetiology, all forms of preeclampsia resolve after delivery of the placenta, confirming central involvement of the organ. In addition, most forms of preeclampsia present with evidence of impaired uteroplacental perfusion and placental hypoxia[2]. However, whether placental hypoxia is merely a consequence of the disease or whether it causes the adverse maternal and fetal outcomes is uncertain. In contrast to the impact of hypoxia on the placenta and fetus, comparatively little is known on the maternal physiology. When investigating interactions among mother, placenta and offspring, maternal metabolism, the temporal profile of fetal development, and access to longitudinal physiological measures are three important considerations. Sheep and humans share a similar precocial profile of organ development, and sheep give birth primarily to singleton or twin lambs of similar weight to humans after a relatively long gestation period[4]. Therefore, the maternal and placental metabolic investment in pregnancy is similar between sheep and humans. In addition, sheep permit longitudinal assessment of uterine blood flow *via* surgically implanted flow probes as well as serial long-term blood sampling for endocrinology[5]. In this study, we have tested the hypothesis that placental hypoxia drives phenotypes of preeclampsia

by investigating the effects on mother, placenta and fetus of chronic hypoxia during late pregnancy. To achieve this, we developed a preclinical model of improved human translational potential to investigate the symptoms of preeclampsia in late gestation in sheep, independent of maladaptive placental changes in early pregnancy.

## Materials & methods

The authors declare that all supporting data are available within the article [and its online supplementary files].

For the purpose of the current study, we exploited recently available novel technology to maintain pregnant sheep under highly controlled isobaric hypoxic conditions, while undergoing wireless recording of maternal cardiovascular function (Figure 1)[6-8]. Then, we combined measurements *in vivo* with functional and molecular analyses to determine the inter-relationship between chronic hypoxia and maternal, placental and fetal outcomes. The experimental design was conducted in accordance with the ARRIVE guidelines[9].

An expanded version of the Materials & Methods is available in the Online Supplement.

## Results

### Chronic hypoxia causes asymmetric fetal growth restriction

Exposure of pregnant ewes to chronic isobaric hypoxia of 10% inspired oxygen for a month from 105 to 138 days gestational age (dGA; term at 145 dGA) was associated with a 28% reduction in fetal growth, decreasing fetal weight from 3.67±0.17kg in normoxic (N) fetuses to 2.65±0.22kg in hypoxic (H) fetuses at 138 dGA (Figure 2A). There was no change in fetal brain weight in H relative to N pregnancies (N: 47.7±0.9 vs. H: 47.8±1.3g). However, when fetal brain weight was expressed relative to fetal body weight, this ratio was significantly increased in H relative to N fetuses (Figure 2B). In contrast, there was no effect of chronic hypoxia on placental weight (Figure 2C) or on the number or weight distribution of different placentome types (Figure S1). These effects of chronic hypoxia on fetal growth occurred in the absence of changes to maternal food intake (Figure S2).

### Chronic hypoxia leads to activation of the placental unfolded protein response

The levels of hypoxia-inducible factor 1α (HIF1α) were greater in H relative to N placentomes at 138 dGA (Figure 3A). The levels of protein carbonylation were greater in H relative to N placentae (Figure 3B), indicative of oxidative stress. This was associated with an increase in the ratio of the phosphorylated forms of the mitogen activated protein kinases C-jun N-terminal kinase (JNK) and the cell survival extracellular signal-regulated kinase (ERK) compared to total levels of these kinases in H relative to N placentae (Figure 3C and 3D). Oxidative protein damage can trigger activation of unfolded protein response (UPR) pathways in different cellular compartments, including the cytosol and endoplasmic reticulum (ER). The UPR signal activator activating transcription factor 6 (ATF6) was increased in H relative to N

placentae (Figure 4A). As part of the endoplasmic reticulum UPR ($UPR^{ER}$), levels of the protein chaperone glucose-related protein 78 (GRP78) and of the protein folding enzyme protein disulfide isomerase (PDI) were higher in H relative to N placentae (Figure 4B). The expression of the cytosolic protein chaperones heat shock protein 27 (HSP27) and heat shock protein 70 (HSP70), part of the cytosolic UPR ($UPR^{Cyt}$), was also greater in H relative to N placentae (Figure 4C). Immunohistochemical analysis showed that ATF6 localised to the nucleus, indicating potential transcriptional activity of ATF6 (Figure 4D). Nuclear staining was more prominent in H compared to N placentae (Figure 4D). Transmission electron microscopy further revealed distended ER morphology in H compared with the ER in N placentae, which displayed a highly defined membrane structure (Figure 4E).

**Chronic hypoxia promotes an angiogenic imbalance in the maternal circulation**

Placental transcripts encoding the anti-angiogenic factors soluble fms-like tyrosine kinase 1 (sFlt-1) and soluble endoglin (sEng), as well as the ratio of the placental transcripts of sFlt-1 compared to the angiogenic factor vascular endothelial growth factor (VEGF), were increased in H relative to N placentae at 138 dGA, as measured by quantitative reverse transcription PCR (Figure 5A-5C). There were no differences in *VEGF* and *PlGF* transcripts, and no differences in the ratio of *sFlt-1* compared to *PlGF* transcripts (Figure S3A-S3C). In N ewes, the concentration of sFlt-1 and the ratios of sFlt-1 to VEGF and to PlGF in plasma did not change in samples taken at baseline and at 138 dGA (Figure 5D-5F). In contrast, in H ewes the concentrations of sFlt-1 and the ratios of sFlt-1 to VEGF and to PlGF were significantly higher at 138 dGA relative to baseline and when compared to values in N ewes at 138 dGA (Figure 5D-5F). Neither N nor H ewes showed changes in sEng, VEGF or PlGF plasma

concentrations with increasing gestation and there were no differences between the groups at baseline or 138 dGA (Figure S3D-S3F).

**Chronic hypoxia increases uteroplacental vascular resistance and prevents the gestational decrease in maternal arterial blood pressure**

At 138 dGA, the uterine artery PI values were greater in H relative to N ewes (Figure 6A). At 138 dGA, independent of treatment, there were significant positive correlations between maternal uterine PI and the maternal plasma sFlt-1 concentration, and between maternal uterine PI and maternal plasma sFlt-1 to PlGF ratio (Figure S4A and S4C). However, there was no correlation between maternal uterine PI and maternal plasma sFlt-1 to VEGF ratio at 138 dGA (Figure S4B). At 138 dGA, plasma creatinine concentrations were slightly higher in H relative to N ewes, which may indicate a reduction in glomerular filtration rate (Figure S5A). However, there was no difference in the urine ratio of albumin to creatinine at 138 dGA (Figure S5B).

Daily changes in maternal arterial blood gas, acid base and metabolic status during exposure to chronic normoxia or chronic hypoxia in the second cohort of animals have been previously reported[7]. In brief, these data confirm a reduction in maternal arterial partial pressure of oxygen ($P_aO_2$) from 105.7±3.7 to 42.0±1.2mmHg and in arterial oxygen saturation 103.5±0.5 to 78.6±5.7% ($P<0.05$) during exposure to chronic isobaric hypoxia of 10% inspired oxygen (Table S1). Ewes exposed to chronic hypoxia had significantly elevated haematocrit and haemoglobin concentration by the end of exposure relative to baseline and to values in N ewes (Table S1). There was no significant change between groups in maternal arterial pH, partial pressure of arterial carbon dioxide, blood glucose or lactate concentrations (Table S1).

Longitudinal continuous measurement of maternal arterial blood pressure and calculation of uterine vascular resistance *via* the wireless CamDAS recording revealed the expected fall in both variables with advancing gestation in N ewes but not in H ewes (Figure 6B and 6C). During baseline conditions, prior to hypoxic exposure, between 122-124 dGA, average values for maternal arterial blood pressure (80.4±1.2 vs. 81.2±3.2mmHg) and for uterine vascular resistance (0.29±0.05 vs. 0.20±0.03mmHg.(ml.min$^{-1}$)$^{-1}$) were not different between N and H ewes. In N pregnancies, values for maternal arterial blood pressure (80.4±1.2 vs. 73.4±1.1mmHg) and for uterine vascular resistance (0.29±0.05 vs. 0.20±0.06mmHg.(ml.min$^{-1}$)$^{-1}$) were significantly lower at 134 dGA compared to earlier in gestation (all $P<0.05$). In contrast, following chronic hypoxic exposure, values for maternal arterial blood pressure (81.2±3.2 vs. 79.6±4.8mmHg) and for uterine vascular resistance (0.20±0.03 vs. 0.19±0.04mmHg.(ml.min-$^{1}$)$^{-1}$) in H pregnancies, were similar at 134 dGA compared to earlier in gestation ($P>0.05$). Maternal arterial blood pressure was not significantly different between N and H pregnancies at 134 dGA.

## Discussion

In the classic two-stage theory of preeclampsia, impaired uteroplacental perfusion promotes placental hypoxia, oxidative stress and ER stress. The subsequent placental release of proinflammatory cytokines, syncytiotrophoblast debris and antiangiogenic factors into the maternal circulation induces the peripheral syndrome[10]. For example, the angiogenic imbalance caused by the release of sFlt-1 and sEng, which oppose the actions of VEGF and PlGF, promotes global maternal endothelial dysfunction and increased peripheral vascular resistance[11]. These changes manifest as an increase in the uterine PI, maternal systemic hypertension and impaired renal glomerular filtration rate[12]. On the fetal side, these changes lead to impaired fetal oxygen and nutrient delivery, yielding asymmetric fetal growth restriction (FGR)[13].

Data in the present study show that chronic hypoxia during the last third of pregnancy in sheep stresses the placenta, with upstream adverse effects on the mother and downstream adverse effects on the fetus, akin to those found in preeclampsia. Placentae from the hypoxic cohort showed molecular evidence of hypoxia, increased oxidative stress, activation of the UPR, dilation of ER cisternae, and increased expression of anti-angiogenic factors. Upstream adverse consequences on the ewe included evidence of an angiogenic imbalance in maternal plasma, increased uterine artery PI and a lack of an ontogenic fall in uterine vascular resistance and arterial blood pressure with advancing gestation. Downstream adverse consequences on the hypoxic offspring included FGR with evidence of fetal brain-sparing. Combined, therefore, the data in this study support the hypothesis that chronic hypoxia during the last third of pregnancy in sheep provides a link between placental stress, FGR and maternal cardiovascular dysfunction in adverse pregnancy, as in preeclampsia.

However, the differences between this pre-clinical model and preeclampsia are just as informative as the similarities. While the data suggest that some features of preeclampsia can be caused by hypoxia, other features, such as overt maternal hypertension and maternal proteinuria, were not recapitulated. However, ewes undergoing hypoxic pregnancy did not show the significant fall in maternal arterial blood pressure measured in control ewes with advancing gestation. Lack of maternal hypertension may therefore be due to the limited duration of hypoxia towards the end of pregnancy in this ovine model. In contrast, in preeclampsia, the pathophysiology can start during the first trimester.

***Chronic hypoxia and asymmetric fetal growth restriction.*** The level of maternal hypoxia used in this model is clinically relevant. Previous studies from our group have used the hypoxic chambers with pregnant sheep, which were surgically prepared with catheters for daily blood sampling and Transonic flow probes for long-term recording of fetal cardiovascular function[7]. These studies revealed that the level of maternal hypoxia used in the present study reduced fetal $P_aO_2$ in the descending aorta to 12mmHg in a highly controlled manner[7]. This level of chronic hypoxia equates to that measured by cordocentesis in human growth restricted fetuses in preeclamptic pregnancies[14]. Our previous studies also revealed that chronic fetal hypoxia promotes a sustained redistribution of blood flow away from the peripheral circulations towards the fetal brain[7,15]. This is the so-called 'fetal brain-sparing effect'[16] and is responsible for the asymmetric FGR measured in chronically hypoxic fetuses both in humans and animal models[15,17]. In the present study, the asymmetric FGR resulting from chronic hypoxia during the last third of pregnancy was represented by a smaller fall in the brain

187 relative to the fetal body weight, yielding an increase in the percentage relative brain
188 weight.

189 ***Chronic hypoxia and placental stress.*** Placental hypoxia promotes an increase in
190 placental oxidative stress[18]. Protein carbonyls are used as biomarkers of reactive
191 oxygen species-mediated protein damage in preeclamptic placentae, and correlate
192 well with the severity of the syndrome[19]. Accumulation of damaged proteins in the
193 placenta is associated with activation of the kinases ERK and JNK, which mediate
194 several responses to cellular stress [20]. As part of the cellular quality control system,
195 the ER ensures protein folding, and is capable of activating a powerful UPR to restore
196 protein homeostasis[21]. In the present study, both the $UPR^{ER}$ and $UPR^{Cyt}$ showed
197 increased activation in hypoxic placentae, along with morphological changes in ER
198 structure. We found that both the expression and nuclear translocation of ATF6 was
199 increased, likely mediating the transcriptional activation of UPR target genes in
200 response to ER stress[22]. In hypoxic placentae the expression of GRP78 and PDI and
201 of HSP27 and HSP70 were increased as part of the $UPR^{ER}$ and the $UPR^{Cyt}$,
202 respectively. Transmission electron microscopy further revealed distended ER cristae
203 in hypoxic placentae. Many of these molecular and morphological markers have been
204 reported in placentae from women suffering from preeclampsia[23-25].

205 ***Chronic hypoxia and maternal adverse effects.*** Healthy human pregnancy is
206 accompanied by a number of maternal cardiovascular adaptations that help support
207 the growing fetus[26]. By mid-gestation, there is a fall in utero-placental vascular
208 resistance, which directs perfusion towards the uterine artery, where blood flow is
209 increased from 20-50 ml/min in the non-pregnant state to 450-800 ml/min[26]. To

accommodate this, the uterine artery markedly increases its diameter, driving a fall in uterine vascular resistance and maternal arterial pressure[27]. Pregnancy at high altitude blunts the rise in uterine blood flow and impairs the fall in maternal arterial blood pressure with advancing gestation in non-indigenous human populations[28,29] and sheep[30,31]. The diminished rise in uterine blood flow in human highland pregnancy is thought to be an important contributor to the enhanced prevalence of preeclampsia and FGR at high altitude[32,33]. Extensive studies by Zhang and colleagues have shown that gestational hypoxia contributes to the maladaptive uterine haemodynamic phenotype through epigenetic regulation of the large conductance calcium-activated potassium channel[30,34].

Data in the present study show that chronic hypoxia during the last third of pregnancy in sheep led to an increase in placental sFlt-1 expression and maternal plasma sFlt-1 concentration. This may be driven by increased placental levels of HIF1α in the hypoxic placenta, which has been previously demonstrated *in vitro* in placental explants and is supported by raised HIF1α levels in the current study[35]. In addition, the fall in uterine vascular resistance and maternal blood pressure with advancing gestation monitored using indwelling flow probes and vascular catheters did not occur in hypoxic ewes. Both uterine vascular dysfunction and increased maternal blood pressure have been reported in sheep undergoing high altitude pregnancy[34]. Therefore, combined, the present study extends previous findings in ovine highland pregnancy[34], highlighting the critical role for oxygen deficiency in placental dysfunction and their relationship with maternal cardiovascular changes. Further, there was a significant positive correlation between maternal uterine PI and the maternal plasma concentration of sFlt-1, and between maternal uterine PI and the maternal plasma

sFlt-1 to PlGF ratio. The data therefore support that increased expression of antiangiogenic factors in the placenta may contribute to an angiogenic imbalance and endothelial dysfunction in the maternal circulation.

**Advances and limitations.** Despite great advances in the understanding of preeclampsia, progress in this field has been hampered by many experimental limitations. While advances such as organoid cultures create new and exciting opportunities, *in vitro* models cannot replicate all *in vivo* interactions between mother, placenta and offspring. On the other hand, there are no preclinical animal models that spontaneously develop preeclampsia, and those available, in which symptoms are induced, have limitations. The same is true for this ovine model of hypoxic pregnancy. Clearly, there are gross anatomical differences between the human haemochorial and the ovine synepitheliochorial placenta[36]. However, there are also important similarities. Both sheep and humans have placental counter-current flow of maternal and fetal blood within the placental villous tree, comparable transplacental oxygen gradients and oxygen consumption rates (37 in sheep vs. 34ml.kg-$^{1}$.min$^{-1}$ in humans), as well as similar nutrient transporter expression[37-41]. At the molecular level, the induction of oxidative and ER stress and the activation of the UPR are highly conserved pathways across species[21]. This is also the case for rodents, in which activation of the placental UPR$^{ER}$ has been demonstrated in hypoxic pregnancy[34].

There have been many other studies by our and other groups in rodent pregnancy investigating the effects of hypoxic pregnancy on the placental phenotype, FGR and on uterine vascular reactivity[42-46]. However, few of these studies have had a focus on placental molecular or maternal circulating markers of preeclampsia or investigated

associated changes in maternal *in vivo* cardiovascular function. It is also important to highlight that the murine placenta is functionally divided into distinct zones for endocrine activity and for nutrient transfer[47]. The labyrinth zone shows high levels of mitochondrial activity, while the junctional zone is less well oxygenated, but prone to ER stress due to its synthetic and secretory activities[48]. Thus, in the murine placenta, crosstalk between ER and mitochondrial stress is limited, with diverging responses depending on which zone is investigated[49,50]. Other murine studies using experimental models of preeclampsia by either eNOS knockout or restriction of uteroplacental perfusion also support a link between placental hypoxia with oxidative stress and impaired placental nutrient transport, FGR and abnormal maternal cardiovascular function[49,51]. This is what we have directly addressed in the present study in an ovine model with increased human translational potential. Nevertheless, extrapolation of these findings to the human clinical condition needs to be viewed with caution.

**Perspectives**

This work introduces a novel large animal model of isobaric hypoxic pregnancy in sheep that not only promotes fetal growth restriction but also recapitulates many of the physiological and molecular features of preeclampsia in the mother and the placenta. These findings are significant, as any changes occur independent of alterations to placentation in early pregnancy. Therefore, the work offers novel ways of thinking about the syndrome and an established platform to develop interventional therapies.

## Article information


### Acknowledgements

W.T. is a PhD student supported by the Centre for Trophoblast Research at the University of Cambridge. We are grateful to the staff of the University of Cambridge Biological Services for helping with the maintenance of the animals at The Barcroft Centre.

### Funding sources

This work was supported by The British Heart Foundation (RG/17/8/32924).


### Competing interests

The authors declare no competing interests.

### Author contributions

Conceptualisation, D.A.G.; Methodology, W.T., B.J.A., K.L.B., O.V.P., Y.N., K.J.B., S.G.F., T.A.G., F.B.P., Q.L., L.Z., J.M., T.C.D., H.W.Y., G.J.B., D.A.G.; Formal Analysis, W.T., B.J.A., K.L.B., O.V.P., Y.N., K.J.B., S.G.F., T.A.G., F.B.P., Q.L., L.Z., J.M., T.C.D., H.W.Y., G.J.B., D.A.G.; .; Writing – Original Draft, W.T., B.J.A., K.L.B., D.A.G.; Writing – Review & Editing, W.T., B.J.A., K.L.B., O.V.P., Y.N., K.J.B., S.G.F., T.A.G., F.B.P., Q.L., L.Z., J.M., T.C.D., H.W.Y., G.J.B.; Visualisation, W.T., D.A.G.; Supervision, W.T., B.J.A., K.L.B., O.V.P., Y.N., K.J.B., S.G.F., T.A.G., F.B.P., Q.L., L.Z., J.M., T.C.D., H.W.Y., G.J.B., D.A.G.; Project Administration, W.T., B.J.A., K.L.B., O.V.P., Y.N., K.J.B., S.G.F., D.A.G.; Funding Acquisition, D.A.G., G.J.B.

## Resource availability

### *Lead contact*

Further information and requests for resources and reagents should be directed to and will be fulfilled by the Lead Contact, Professor Dino A. Giussani (dag26@cam.ac.uk).

### *Materials availability*

This study did not generate new unique reagents.

### *Data and code availability*

This study did not generate/analyse any datasets or code

## References


1. Gynecologists ACoOa. Gestational Hypertension and Preeclampsia: ACOG Practice Bulletin, Number 222. Paper/Poster presented at: Obstetrics & Gynecology; 2020;
2. Steegers EAP, von Dadelszen P, Duvekot JJ, Pijnenborg R. Pre-eclampsia. *The Lancet*. 2010;376:631-644. doi: https://doi.org/10.1016/S0140-6736(10)60279-6
3. Burton GJ, Redman CW, Roberts JM, Moffett A. Pre-eclampsia: pathophysiology and clinical implications. *BMJ*. 2019;366:l2381. doi: 10.1136/bmj.l2381
4. Barry JS, Anthony RV. The Pregnant Sheep as a Model for Human Pregnancy. *Theriogenology*. 2008;69:55-67. doi: 10.1016/j.theriogenology.2007.09.021
5. Jellyman JK, Gardner DS, Fowden AL, Giussani DA. Effects of dexamethasone on the uterine and umbilical vascular beds during basal and hypoxemic conditions in sheep. *American journal of obstetrics and gynecology*. 2004;190:825-835. doi: 10.1016/j.ajog.2003.09.046
6. Brain KL, Allison BJ, Niu Y, Cross CM*, et al.* Induction of controlled hypoxic pregnancy in large mammalian species. *Physiological Reports*. 2015;3:e12614. doi: doi:10.14814/phy2.12614
7. Allison BJ, Brain KL, Niu Y, Kane AD*, et al.* Fetal in vivo continuous cardiovascular function during chronic hypoxia. *The Journal of Physiology*. 2016;594:1247-1264. doi: 10.1113/JP271091
8. Shaw CJ, Allison BJ, Itani N, Botting KJ*, et al.* Altered autonomic control of heart rate variability in the chronically hypoxic fetus. *The Journal of Physiology*. 2018;596:6105-6119. doi: 10.1113/jp275659

9. Kilkenny C, Browne WJ, Cuthill IC, Emerson M*, et al.* Improving Bioscience Research Reporting: The ARRIVE Guidelines for Reporting Animal Research. *PLoS Biology*. 2010;8:e1000412. doi: 10.1371/journal.pbio.1000412

10. Tong W, Giussani DA. Preeclampsia link to gestational hypoxia. *Journal of developmental origins of health and disease*. 2019;10:322-333. doi: 10.1017/S204017441900014X

11. Powe CE, Levine RJ, Karumanchi SA. Preeclampsia, a disease of the maternal endothelium: the role of antiangiogenic factors and implications for later cardiovascular disease. *Circulation*. 2011;123:2856-2869. doi: 10.1161/CIRCULATIONAHA.109.853127

12. VanWijk MJ, Kublickiene K, Boer K, VanBavel E. Vascular function in preeclampsia. *Cardiovascular research*. 2000;47:38-48. doi: 10.1016/S0008-6363(00)00087-0

13. Poston L. The control of blood flow to the placenta. *Experimental Physiology*. 1997;82:377-387. doi: doi:10.1113/expphysiol.1997.sp004033

14. Nicolaides KH, Rodeck CH, Soothill PW, Campbell S. Ultrasound-guided sampling of umbilical cord and placental blood to assess fetal wellbeing *The Lancet*. 1986;327:1065-1067. doi: https://doi.org/10.1016/S0140-6736(86)91333-4

15. Giussani DA. Breath of Life: Heart Disease Link to Developmental Hypoxia. *Circulation*. 2021;144:1429-1443. doi: 10.1161/CIRCULATIONAHA.121.054689

16. Giussani DA. The fetal brain sparing response to hypoxia: physiological mechanisms. *The Journal of physiology*. 2016;594:1215-1230. doi: 10.1113/JP271099

17. Swanson AM, David AL. Animal models of fetal growth restriction: Considerations for translational medicine. *Placenta*. 2015;36:623-630. doi: 10.1016/j.placenta.2015.03.003

18. Sferruzzi-Perri AN, Higgins JS, Vaughan OR, Murray AJ*, et al.* Placental mitochondria adapt developmentally and in response to hypoxia to support fetal growth. *Proc Natl Acad Sci U S A*. 2019;116:1621-1626. doi: 10.1073/pnas.1816056116

19. Zusterzeel PLM, Rütten H, Roelofs HMJ, Peters WHM*, et al.* Protein Carbonyls in Decidua and Placenta of Pre-eclamptic Women as Markers for Oxidative Stress. *Placenta*. 2001;22:213-219. doi: https://doi.org/10.1053/plac.2000.0606

20. Tang C, Liang J, Qian J, Jin L*, et al.* Opposing role of JNK-p38 kinase and ERK1/2 in hydrogen peroxide-induced oxidative damage of human trophoblast-like JEG-3 cells. *International Journal of Clinical and Experimental Pathology*. 2014;7:959-968.

21. Schröder M, Kaufman RJ. The mammalian unfolded protein response. *Annual Review of Biochemistry*. 2005;74:739-789. doi: 10.1146/annurev.biochem.73.011303.074134

22. Adams CJ, Kopp MC, Larburu N, Nowak PR*, et al.* Structure and Molecular Mechanism of ER Stress Signaling by the Unfolded Protein Response Signal Activator IRE1. *Frontiers in Molecular Biosciences*. 2019;6. doi: 10.3389/fmolb.2019.00011

23. Charnock-Jones DS. Placental hypoxia, endoplasmic reticulum stress and maternal endothelial sensitisation by sFLT1 in pre-eclampsia. *Journal of*

*Reproductive Immunology*. 2016;114:81-85. doi: https://doi.org/10.1016/j.jri.2015.07.004

24. Yung HW, Cox M, Tissot van Patot M, Burton GJ. Evidence of endoplasmic reticulum stress and protein synthesis inhibition in the placenta of non-native women at high altitude. *FASEB J*. 2012;26:1970-1981. doi: 10.1096/fj.11-190082

25. Yung HW, Atkinson D, Campion-Smith T, Olovsson M*, et al.* Differential activation of placental unfolded protein response pathways implies heterogeneity in causation of early- and late-onset pre-eclampsia. *The Journal of Pathology*. 2014;234:262-276. doi: 10.1002/path.4394

26. Palmer SK, Zamudio S, Coffin C, Parker S*, et al.* Quantitative estimation of human uterine artery blood flow and pelvic blood flow redistribution in pregnancy. *Obstetrics and gynecology*. 1992;80:1000-1006.

27. Kublickiene KR, Cockell AP, Nisell H, Poston L. Role of nitric oxide in the regulation of vascular tone in pressurized and perfused resistance myometrial arteries from term pregnant women. *Am J Obstet Gynecol*. 1997;177:1263-1269. doi: 10.1016/s0002-9378(97)70048-6

28. Palmer SK, Moore LG, Young D, Cregger B*, et al.* Altered blood pressure course during normal pregnancy and increased preeclampsia at high altitude (3100 meters) in Colorado. *Am J Obstet Gynecol*. 1999;180:1161-1168. doi: 10.1016/s0002-9378(99)70611-3

29. Giussani DA, Salinas CE, Villena M, Blanco CE. The role of oxygen in prenatal growth: studies in the chick embryo. *The Journal of physiology*. 2007;585:911-917. doi: 10.1113/jphysiol.2007.141572

30. Hu X-Q, Chen M, Dasgupta C, Xiao D*, et al.* Chronic hypoxia upregulates DNA methyltransferase and represses large conductance Ca2+-activated K+ channel function in ovine uterine arteries. *Biology of reproduction*. 2017;96:424-434. doi: 10.1095/biolreprod.116.145946

31. Ducsay CA, Goyal R, Pearce WJ, Wilson S*, et al.* Gestational Hypoxia and Developmental Plasticity. *Physiological reviews*. 2018;98:1241-1334. doi: 10.1152/physrev.00043.2017

32. Keyes LE, Armaza JF, Niermeyer S, Vargas E*, et al.* Intrauterine growth restriction, preeclampsia, and intrauterine mortality at high altitude in Bolivia. *Pediatr Res*. 2003;54:20-25. doi: 10.1203/01.PDR.0000069846.64389.DC

33. Julian CG, Galan HL, Wilson MJ, Desilva W*, et al.* Lower uterine artery blood flow and higher endothelin relative to nitric oxide metabolite levels are associated with reductions in birth weight at high altitude. *Am J Physiol Regul Integr Comp Physiol*. 2008;295:R906-915. doi: 10.1152/ajpregu.00164.2008

34. Hu X-Q, Dasgupta C, Xiao D, Huang X*, et al.* MicroRNA-210 Targets Ten-Eleven Translocation Methylcytosine Dioxygenase 1 and Suppresses Pregnancy-Mediated Adaptation of Large Conductance Ca(2+)-Activated K(+) Channel Expression and Function in Ovine Uterine Arteries. *Hypertension (Dallas, Tex : 1979)*. 2017:HYPERTENSIONAHA.117.09864. doi: 10.1161/HYPERTENSIONAHA.117.09864

35. Iwagaki S, Yokoyama Y, Tang L, Takahashi Y*, et al.* Augmentation of leptin and hypoxia-inducible factor 1α mRNAs in the pre-eclamptic placenta. *Gynecological Endocrinology*. 2004;18:263-268. doi: 10.1080/09513590420000196277

36. Wooding FBP, Burton G. *Comparative Placentation: Structures, Functions and Evolution*. 2008.

37. Wilkening RB, Molina RD, Meschia G. Placental oxygen transport in sheep with different hemoglobin types. *American Journal of Physiology-Regulatory, Integrative and Comparative Physiology*. 1988;254:R585-R589. doi: 10.1152/ajpregu.1988.254.4.R585

38. Bonds DR, Crosby LO, Cheek TG, Hägerdal M*, et al.* Estimation of human fetal-placental unit metabolic rate by application of the Bohr principle. *Journal of developmental physiology*. 1986;8:49-54.

39. Ma Y, Zhu MJ, Uthlaut AB, Nijland MJ*, et al.* Upregulation of growth signaling and nutrient transporters in cotyledons of early to mid-gestational nutrient restricted ewes. *Placenta*. 2011;32:255-263. doi: 10.1016/j.placenta.2011.01.007

40. Regnault TRH, de Vrijer B, Galan HL, Wilkening RB*, et al.* Umbilical uptakes and transplacental concentration ratios of amino acids in severe fetal growth restriction. *Pediatric Research*. 2013;73:602. doi: 10.1038/pr.2013.30

41. Hafez SA, Borowicz P, Reynolds LP, Redmer DA. Maternal and fetal microvasculature in sheep placenta at several stages of gestation. *J Anat*. 2010;216:292-300. doi: 10.1111/j.1469-7580.2009.01184.x

42. Nuzzo AM, Camm EJ, Sferruzzi-Perri AN, Ashmore TJ*, et al.* Placental Adaptation to Early-Onset Hypoxic Pregnancy and Mitochondria-Targeted Antioxidant Therapy in a Rodent Model. *The American Journal of Pathology*. 2018;188:2704-2716. doi: https://doi.org/10.1016/j.ajpath.2018.07.027

440 43. Skeffington KL, Higgins JS, Mahmoud AD, Evans AM*, et al.* Hypoxia, AMPK
441 activation and uterine artery vasoreactivity. *The Journal of physiology*.
442 2016;594:1357-1369. doi: 10.1113/JP270995
443 44. Matheson H, Veerbeek JH, Charnock-Jones S, Burton GJ*, et al.* Morphological
444 and molecular changes in the murine placenta exposed to normobaric hypoxia
445 throughout pregnancy. *The Journal of Physiology*. 2016;594:1371-1388. doi:
446 10.1113/JP271073
447 45. Higgins JS, Vaughan OR, Fernandez de Liger E, Fowden AL*, et al.* Placental
448 phenotype and resource allocation to fetal growth are modified by the timing
449 and degree of hypoxia during mouse pregnancy. *The Journal of physiology*.
450 2016;594:1341-1356. doi: 10.1113/JP271057
451 46. Camm EJ, Hansell JA, Kane AD, Herrera EA*, et al.* Partial contributions of
452 developmental hypoxia and undernutrition to prenatal alterations in somatic
453 growth and cardiovascular structure and function. *American Journal of*
454 *Obstetrics and Gynecology*. 2010;203:495.e424-495.e434. doi:
455 https://doi.org/10.1016/j.ajog.2010.06.046
456 47. Woods L, Perez-Garcia V, Hemberger M. Regulation of Placental Development
457 and Its Impact on Fetal Growth-New Insights From Mouse Models. *Front*
458 *Endocrinol (Lausanne)*. 2018;9:570-570. doi: 10.3389/fendo.2018.00570
459 48. Yung HW, Colleoni F, Dommett E, Cindrova-Davies T*, et al.* Noncanonical
460 mitochondrial unfolded protein response impairs placental oxidative
461 phosphorylation in early-onset preeclampsia. *Proceedings of the National*
462 *Academy of Sciences*. 2019;116:18109-18118. doi: 10.1073/pnas.1907548116
463 49. Kusinski LC, Stanley JL, Dilworth MR, Hirt CJ*, et al.* eNOS knockout mouse as
464 a model of fetal growth restriction with an impaired uterine artery function and

placental transport phenotype. *American Journal of Physiology-Regulatory, Integrative and Comparative Physiology*. 2012;303:R86-R93. doi: 10.1152/ajpregu.00600.2011

50. Burton GJ, Yung HW, Murray AJ. Mitochondrial – Endoplasmic reticulum interactions in the trophoblast: Stress and senescence. *Placenta*. 2017;52:146-155. doi: https://doi.org/10.1016/j.placenta.2016.04.001

51. Amaral LM, Pinheiro LC, Guimaraes DA, Palei ACT*, et al.* Antihypertensive effects of inducible nitric oxide synthase inhibition in experimental pre-eclampsia. *Journal of cellular and molecular medicine*. 2013;17:1300-1307. doi: 10.1111/jcmm.12106

## Novelty and Relevance

### What is new?

- A common feature of preeclampsia is placental hypoxia. However, whether placental hypoxia is merely a consequence of the disease or whether it causes the adverse maternal and fetal outcomes is uncertain.
- Here, we show using a novel *in vivo* approach that placental hypoxia drives maternal and fetal phenotypes associated with preeclampsia.

### What is relevant?

- Pregnancy affected by uteroplacental hypoxia, one of the most common pregnancy complications leading to fetal growth restriction in humans, increases the risk of physiological and molecular markers of preeclampsia.

### Clinical and pathophysiological implications?

- Chronic hypoxia in ovine pregnancy recapitulates markers of preeclampsia in the mother, placenta and offspring, indicating that placental hypoxia is an initiating factor in the pathoaetiology of preeclampsia.
- Therefore, biomarkers of placental hypoxia, oxidative stress and activation of the unfolded protein response must be addressed to guide future clinical management of preeclampsia.

## Figure Legends

***Figure 1. Isobaric hypoxic chambers and wireless recording CamDAS$^{TM}$ system.*** *Both panels: A specially designed nitrogen-generating system supplied compressed air and nitrogen to the bespoke isobaric hypoxic chambers housed at The Barcroft Centre, University of Cambridge. Each chamber was equipped with an electronic servo-controlled humidity cool steam injection system to return the appropriate humidity to the inspirate (i). Ambient partial pressures of oxygen and carbon dioxide, humidity, and temperature within each chamber were monitored via sensors (ii). For experimental procedures, each chamber had a double transfer port (iii) to internalise material and a manually operated sliding panel (iv) to bring the ewe into a position, where daily sampling of blood could be achieved through glove compartments (v). Each chamber incorporated a drinking bowl on continuous water supply and a rotating food compartment (vi) for determining food intake. A sealed transfer isolation cart could be attached to a side exit (vii) to couple chambers together for cleaning. Waste could be disposed via a sealable pipe (viii). Panel B: A separate cohort of ewes was instrumented with the CamDAS$^{TM}$ system during surgery, allowing continuous longitudinal monitoring of arterial blood pressure and uterine blood flow. The wireless CamDAS$^{TM}$ system was contained in two parts in a custom-made sheep jacket: the data acquisition box (ix) on one side and a box containing the pressure transducers (x) on the other side. Cables (xi) provided connection between the two boxes and to two battery packs. Measurements made using the CamDAS$^{TM}$ system were transmitted wirelessly via Bluetooth technology (xiii) to a laptop on the outside (xii), on which it was possible to continuously measure and record uterine blood flow and maternal arterial blood pressure during the experimental period (reproduced with permission[6,7]).*

***Figure 2. Hypoxic pregnancy causes asymmetric FGR.*** *Values are mean ± SEM for fetal weight (A), the ratio of fetal brain to body weight (B) and placental weight (C). Groups are N (○,n=9-13) and H (●,n=7-8). Significant differences (P<0.05) are *N vs. H, Student's t-test for unpaired data.*

***Figure 3. Hypoxic pregnancy activates the placental stress response.*** *Values are mean ± SEM for the relative ratio of placental levels of HIF1α (A), of protein carbonylation (B), of the ratio of phosphorylated to total stress kinases JNK (C) and ERK (D). Blots for JNK and ERK appear atypical as they were resolved on 14% agarose gels for higher resolution. Groups are N (○,n=9-10) and H (●,n=7). Significant differences (P<0.05) are *N vs. H, Student's t-test for unpaired data.*

***Figure 4. Hypoxic pregnancy activates the placental UPR response.*** *Values are mean ± SEM for the relative ratio of the placental levels of ATF6 (A), GRP78 and PDI (B) and HSP27 and HSP70 (C). Groups are N (○,n=9-10) and H (●,n=7). Significant differences (P<0.05) are *N vs. H, Student's t-test for unpaired data. In the placenta, ATF6 localises to the nuclei (D), with more prominent nuclear staining in H compared to N placentae. Pictured (D): trophoblast containing binucleate cells (arrows); scale bar = 50μm. Change in trophoblast ER structure was examined by transmission electron microscopy (E). Representative images taken at 5,000x magnification are shown. Arrows indicate the location of ER and stars indicate the location of the nucleus; scale bar = 500nm.*

***Figure 5. Hypoxic pregnancy changes placental expression of anti-angiogenic factors, increasing the anti- to pro-angiogenic balance in maternal plasma.*** *Upper panel: Values are mean ± SEM for the relative placental fold change for sFlt-1 (A), sEng (B) and the ratio of sFlt-1 to VEGF (C) . Lower panel: Values are mean ± SEM for plasma concentration of sFlt-1 (D) and plasma ratios of sFlt-1 to PlGF (E) and to VEGF (F) . Groups are N (○,n=7-9) and H (●,n=7). Significant differences (P<0.05) are *N vs. H or † vs baseline; Student's t-test for unpaired data or two-way RM-ANOVA where appropriate.*

***Figure 6. Hypoxic pregnancy causes maternal cardiovascular dysfunction.*** *Values are mean ± SEM for uterine artery PI (A) and the change from baseline in uterine vascular resistance (B) and in arterial blood pressure (C). Groups are N (○,n=5-9), H (●,n=5-7). Significant differences (P<0.05) are *N vs. H, or † vs baseline; Student's t-test for unpaired data or two-way RM-ANOVA, where appropriate.*

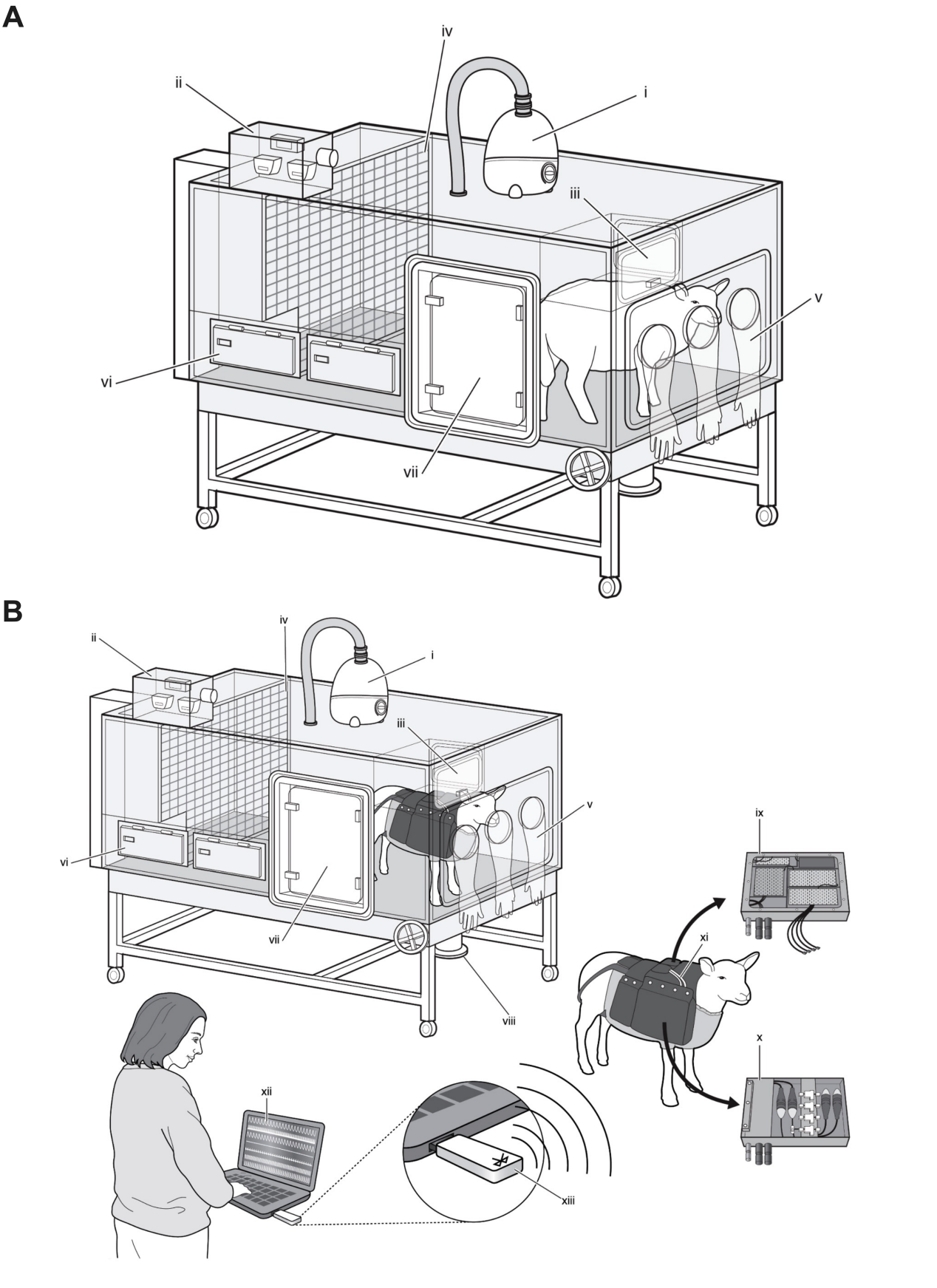
A
ii
iv
i
iii
v
vi
vii
B
ii
iv
i
iii
v
vi
vii
viii
ix
xi
x
xii
xiii

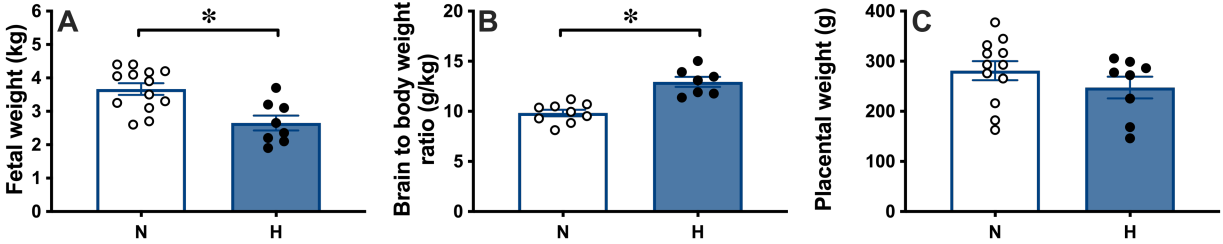
Fetal weight
A
Fetal weight (kg)
6
5
4
3
2
1
0
*
N
H
Asymmetric FGR
B
Brain to body weight ratio (g/kg)
20
15
10
5
0
*
N
H
Placental weight
C
Placental weight (g)
400
300
200
100
0
N
H

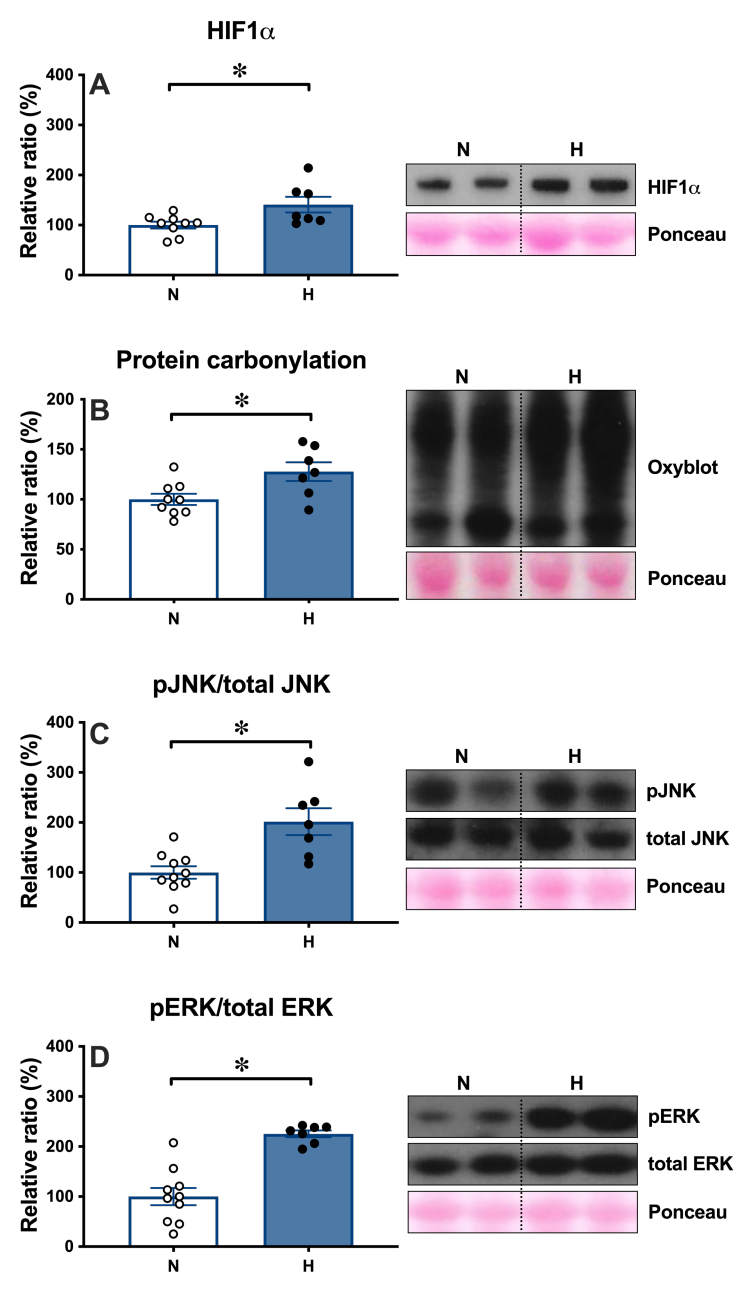
HIF1α
A
Relative ratio (%)
400
300
200
100
0
*
N
H
N
H
HIF1α
Ponceau
Protein carbonylation
B
Relative ratio (%)
200
150
100
50
0
*
N
H
N
H
Oxyblot
Ponceau
pJNK/total JNK
C
Relative ratio (%)
400
300
200
100
0
*
N
H
N
H
pJNK
total JNK
Ponceau
pERK/total ERK
D
Relative ratio (%)
400
300
200
100
0
*
N
H
N
H
pERK
total ERK
Ponceau

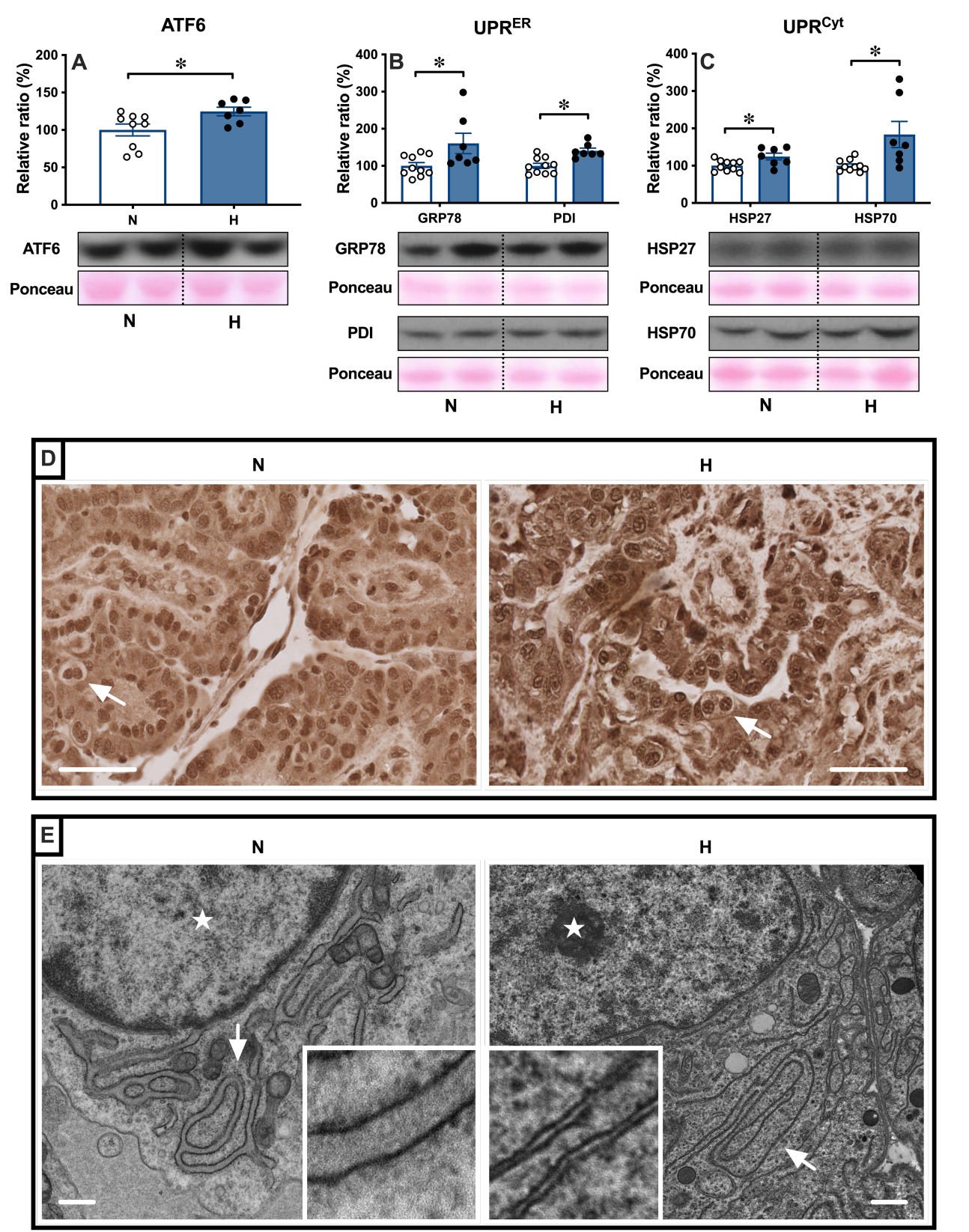
ATF6
UPR^ER
UPR^Cyt
A
B
C
Relative ratio (%)
200
150
100
50
0
400
300
200
100
0
*
N
H
GRP78
PDI
HSP27
HSP70
ATF6
Ponceau
GRP78
PDI
HSP27
HSP70
D
E

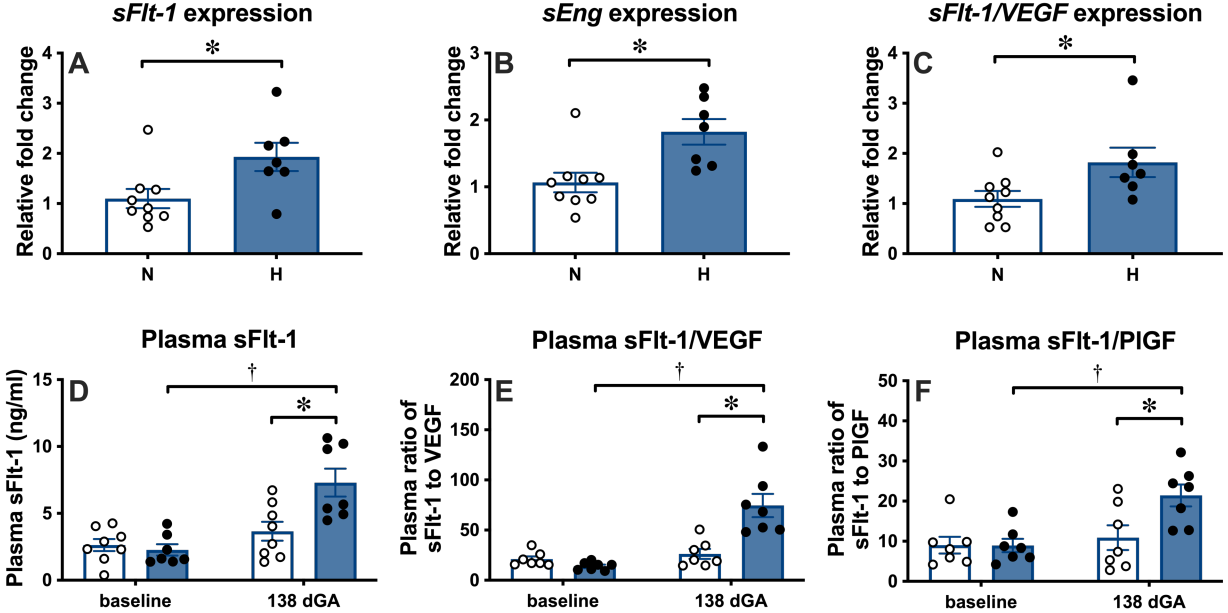
sFlt-1 expression
A
Relative fold change
0
1
2
3
4
*
N
H
sEng expression
B
Relative fold change
0
1
2
3
*
N
H
sFlt-1/VEGF expression
C
Relative fold change
0
1
2
3
4
*
N
H
Plasma sFlt-1
D
Plasma sFlt-1 (ng/ml)
0
5
10
15
†
*
baseline
138 dGA
Plasma sFlt-1/VEGF
E
Plasma ratio of sFlt-1 to VEGF
0
50
100
150
200
†
*
baseline
138 dGA
Plasma sFlt-1/PlGF
F
Plasma ratio of sFlt-1 to PlGF
0
10
20
30
40
50
†
*
baseline
138 dGA

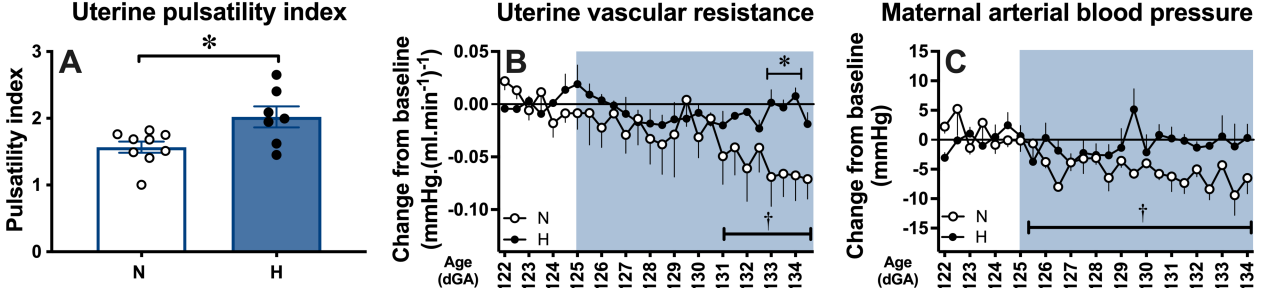
Uterine pulsatility index
A
Pulsatility index
3
2
1
0
*
N
H
Uterine vascular resistance
B
Change from baseline (mmHg.(ml.min-1)-1)
0.05
0.00
-0.05
-0.10
*
†
N
H
Age (dGA)
122
123
124
125
126
127
128
129
130
131
132
133
134
Maternal arterial blood pressure
C
Change from baseline (mmHg)
15
10
5
0
-5
-10
-15
†
N
H
Age (dGA)
122
123
124
125
126
127
128
129
130
131
132
133
134

# New model to understand and treat preeclampsia

**Hypoxic pregnancy**

**Preeclampsia**

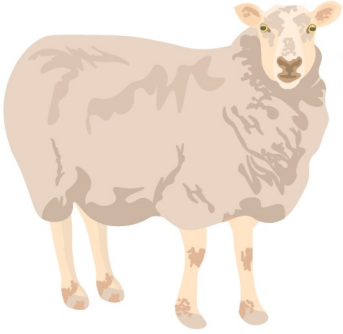

**SHARED PATHOLOGY**

Fetal growth restriction

Anti-angiogenic phenotype

Oxidative damage

Activated stress response pathways

Altered maternal blood pressure

Altered maternal kidney function

Increased uterine vascular resistance

# Chronic hypoxia in ovine pregnancy recapitulates physiological and molecular markers of preeclampsia in the mother, placenta and offspring

Wen Tong[1,2], Beth J. Allison[1], Kirsty L. Brain[1], Olga V. Patey[1], Youguo Niu[1-5], Kimberley J. Botting[1-4], Sage G. Ford[1], Tess A. Garrud[1,2], Peter F. B. Wooding[1,2], Caroline J. Shaw[6], Qiang Lyu[5], Lin Zhang[5], Jin Ma[5], Tereza Cindrova-Davies[1-3], Hong Wa Yung[1-3], Graham J. Burton[1-3], Dino A. Giussani*[1-5]

[1]*Department of Physiology Development & Neuroscience, University of Cambridge, United Kingdom;*

[2]*Centre for Trophoblast Research, University of Cambridge, United Kingdom*;

[3]*Strategic Research Initiative in Reproduction, University of Cambridge, United Kingdom*

[4]*BHF Cardiovascular Centre for Research Excellence, University of Cambridge, United Kingdom*

[5]*Department of Aerospace Physiology, Fourth Military Medical University, Xi'an, China;*

[6]*Department of Metabolism, Digestion and Reproduction, Imperial College London, United Kingdom*

**Short Title**: Pre-eclampsia link to gestational hypoxia

**Corresponding Author**: Professor Dino A. Giussani PhD ScD FRCOG
Department of Physiology, Development and Neuroscience
University of Cambridge
Downing Street, Cambridge
CB2 3EG, UK
Email: dag26@cam.ac.uk
Tel: +44 (0)1223 333894

*Online supplement*

# Expanded Materials & Methods

### *Ethical approval*

All procedures were performed at The Barcroft Centre of The University of Cambridge under the UK Animals Scientific Procedures Act 1986 and were approved by the Ethical Review Board of the University of Cambridge. The experimental design was conducted in accordance with the ARRIVE guidelines [1].

### *Exposure to chronic hypoxia*

Pregnant Welsh mountain ewes carrying singleton fetuses determined by ultrasound scan at 80 days gestational age (dGA; Toshiba Medical Systems Europe, Zoetermeer, Netherlands; term is *ca.* 145 days) were randomly assigned at 103 dGA to either chronic normoxia (N) or chronic hypoxia (H). From 103 dGA, N and H ewes were fed daily a bespoke maintenance diet consisting of concentrate and hay pellets, thereby facilitating the monitoring of food intake (Cambridge ewe diet: 40g nuts/kg and 3g hay/kg; Manor Farm Feeds Ltd; Oakham, Leicestershire, UK). At 103 dGA, H ewes were moved into one of four bespoke isobaric hypoxic chambers (Telstar Ace, Dewsbury, West Yorkshire, UK; Figure 1A in main text) housed in a laboratory. Ewes assigned to chronic normoxia were housed in individual floor pens with the same floor area as the hypoxic chambers. The hypoxic chambers were supplied with controlled volumes of nitrogen and air via a bespoke air and nitrogen generating system (Domnick Hunter Gas Generation, Gateshead, Tyne & Wear, UK), as previously described in detail [2-4]. In brief, compressed air and compressed nitrogen were piped to the laboratory and gases were mixed to requirements via flow metres prior to entering the chambers. The inspirate was passed via silencers able to reduce noise to levels below regulation, providing a tranquil environment for the animal inside each chamber. The volume of gas in each chamber underwent a minimum of 12 changes per hour. All chambers were equipped with humidifiers (1100-03239 HS-SINF Masalles, Barcelona, Spain) and ambient $PO_2$, $PCO_2$, humidity and temperature within each chamber were monitored via sensors and values recorded continuously via the Trends Building Management System of the University of Cambridge. In this way, the level of oxygen within each chamber could be controlled with precision longitudinally over long periods of time. At 105 dGA, H ewes were gradually subjected to hypoxia, reaching 10 ± 1% inspired oxygen over 24h. This level of hypoxia was maintained for a month until 138dGA. For blood sampling procedures during this period, materials could be introduced into the chambers via a double transfer port. A sliding panel was then manually operated, encouraging the ewe to the front of the chamber, which permitted blood samples to be taken via glove compartments using sterile techniques and without losing the hypoxic exposure (Figure 1). In both N and H ewes, venous samples (5 ml) were taken from the jugular vein at 103 and 105 dGA (baseline) and at 138 dGA (end of chronic exposure). Samples were centrifuged, snap frozen in liquid nitrogen and stored at -80 ºC for subsequent analysis.

### *Doppler ultrasonography*

At 138 dGA, following blood sampling, N and H ewes were moved to a nearby ultrasound room. Ultrasonography was performed using a Toshiba Powervision 7000

System with a convex 3.75 MHz Toshiba PVK-357AT transducer. Colour Doppler was used to identify the uterine artery, and the uterine artery PI was calculated using colour Doppler flowmetry. An average value of three consecutive waveforms on both uterine arteries was used for analysis. Ewes in the H group were transported to the ultrasound room and underwent all ultrasound procedures maintaining the hypoxic exposure of 10 ± 1% inspired oxygen via a customised respiratory hood in a mobile cart unit. The gas mixture supplying the respiratory hood was the same ratio as the gas mixture of air and nitrogen supplying the chambers, adjusted to volume.

### *Post-mortem, tissue and urine collection*

At 138 dGA, following ultrasonography, N and H ewes were moved to the post-mortem laboratory. Ewes in the H group remained hypoxic at 10 ± 1% inspired oxygen via the respiratory hood until euthanasia. Both N and H ewes were killed humanely by an overdose of sodium pentobarbitone (0.4 ml/kg intravenously, Pentoject; Animal Ltd., UK). A urine sample (5 ml) was taken with a syringe and needle via puncture directly from the bladder. The fetus was delivered by hysterotomy, weighed and measured. One group of scientists isolated the maternal and fetal organs, which were weighed and fixed in 4% paraformaldehyde or snap frozen in liquid nitrogen and stored at -80°C until further analysis.
Following hysterectomy, individual placentomes were isolated, weighed and counted. Typed placentomes were counted and weighed, and placentomes of each type were also fixed or frozen for further analysis. The distribution of different types of placentomes was not different between N and H pregnancies (Figure S1). For consistency, all placental analysis was performed on type A placentomes.

### *Placental studies*

***Measurement of protein carbonylation***. Flash frozen A-type placentomes were homogenised to powder using pestle and mortar while keeping tissues frozen on dry ice. Homogenates and ice-cold cell lysis buffer (1 mL of buffer per 100 mg of tissue; Cell Signaling Technology, UK) containing protease inhibitors (Roche Diagnostics, UK) were used to prepare protein lysates. Protein concentration was determined using a bicinchoninic acid assay (Thermo Fisher Scientific, UK). To determine post-translational protein carbonylation as a result of oxidative damage, an OxyBlot™ analysis was performed, according to the manufacturer's instructions (Millipore, Billerica, MA). In short, protein lysates were treated to derivatise carbonyl groups to 2,4-dinitrophenyl-hydrazone moieties, separated by 12% sodium dodecyl sulfate polyacrylamide gel electrophoresis and then transferred onto a nitrocellulose membrane (Hybond® ECL™, Sigma-Aldrich, UK). Non-specific binding was inhibited by blocking the membrane in 2.5% bovine serum albumin in Tris-buffered saline containing 0.1% Tween 20 (TBS-T) for 1 h at room temperature. The nitrocellulose membrane was incubated with a primary rabbit anti-2,4-dinitrophenyl-hydrazone antibody (Chemicon Oxyblot™; diluted 1:200) for 1 h at room temperature. Following incubation with the primary antibody, membranes were washed with TBS-T and incubated with a secondary antibody conjugated with horseradish peroxidase against Rabbit IgG (Thermo Fisher, UK; diluted 1:10000) for 1 h at room temperature. Following further washing with TBS-T, protein levels were visualised using an enhanced chemiluminescence kit (Pierce™ ECL, Thermo Fisher Scientific, UK). Protein band densities were quantified using ImageJ software (NIH, RRID:SCR_003070) and normalised against Ponceau S staining.

***Western blotting.*** To determine placental protein expression, whole cell lysates were prepared from homogenates of flash frozen A-type placentomes. This was performed using ice-cold cell lysis buffer (1 mL of buffer per 100 mg of tissue; Cell Signaling Technology, UK) containing protease inhibitors (Roche Diagnostics, UK). Protein concentration was determined using a bicinchoninic acid assay (Thermo Fisher Scientific, UK). Samples were mixed with sodium dodecyl sulfate gel loading buffer and denatured for five minutes at 70 ºC. 15-30 µg aliquots of protein were resolved on 10-12% sodium dodecyl sulfate polyacrylamide gel electrophoresis agarose gels, transferred onto nitrocellulose membranes (Hybond® ECL™, Sigma-Aldrich, UK) and stained with 0.1% Ponceau S in 5% acetic acid (Sigma-Aldrich, UK). Non-specific binding was inhibited by blocking the membrane in 5% dry skim milk in TBS-T for 1 h at room temperature. Following incubation with the primary antibody, membranes were washed with TBS-T and incubated with the relevant secondary antibodies conjugated with horseradish peroxidase against Rabbit IgG (Thermo Fisher, UK; diluted 1:10,000) or against Mouse IgG (Thermo Fisher, UK; diluted 1:10,000) for 1 h at room temperature, where appropriate. Following further washing with TBS-T, protein levels were visualised using an enhanced chemiluminescence kit (Pierce™ ECL, Thermo Fisher Scientific, UK) on film (Amersham™ Hyperfilm™ ECL, GE Healthcare, UK). Protein band densities were quantified using ImageJ software (NIH; RRID:SCR_003070) and normalised against Ponceau S staining. A full list of primary antibodies, dilutions and incubation times can be found in the Major Resources Table.

***Immunohistochemistry*.** Formalin-fixed paraffin-embedded A-type placentomes were sectioned to 7 µm thickness using a microtome (Leica Biosystems, UK) and mounted onto Superfrost™ Plus microscope slides and incubated at 37 ºC overnight. Sections were rehydrated in tap water for 10 minutes and incubated in 3% hydrogen peroxide (Fisher Scientific) for 15 minutes to block endogenous peroxidase activity. After rinsing in distilled water, the sections were incubated in Tris-buffered saline containing 0.1% Tween 20 and 0.1% Triton X-100 (TBS-TT) for 30 minutes. After rinsing in Tris-buffered saline (TBS), slides were blocked in 5% bovine serum albumin in TBS for 1 hour and then incubated overnight in primary antibody against ATF6 (Abcam, UK; ab37149; RRID:AB 725571; diluted 1:200) in 5% bovine serum albumin. The following day, sections were washed using TBS-TT and then incubated in biotinylated secondary antibody against Rabbit IgG (Vector Laboratories, Canada; diluted 1:200) in 5% bovine serum albumin. After washing in TBS-TT, staining was visualised using the VECTASTAIN avidin-biotin complex method (Vector Laboratories, Canada) by adding metal DAB (Thermo Fisher Scientific, UK) as the chromogen for 5 minutes. Staining was stopped by rinsing in distilled water. Sections were dehydrated, and cover slips mounted using DPX Mountant (Sigma-Aldrich, UK).

***Transmission Electron Microscopy***. Tissue processing, embedding and sectioning was performed by the Cambridge Advanced Imaging Centre. In brief, small pieces of A-type placentome tissue were fixed by immersion in 2 mM calcium chloride in 0.05M Sodium cacodylate buffer at pH 7.4 containing 2% glutaraldehyde and 2% formaldehyde. The tissues were fixed overnight at 4°C and osmicated in 0.05M Sodium cacodylate buffer at pH 7.4 containing 1% osmium tetroxide and 1.5% potassium ferricyanide for three days at 4°C. They were treated with 0.1% thiocarbohydrazide for 20 min in the dark at room temperature. They were then osmicated a second time in 2% osmium tetroxide and stained in 0.05 maleate buffer

at pH 5.5 containing 2% uranyl acetate for three days at 4°C. The tissue was dehydrated in ascending concentrations to 100% ethanol and then in 100% dry acetone and dry acetonitrile. They were embedded in Quetol epoxy resin over the course of 11 days. 80 nm sections were cut on a Ultracut UCT (Leica, Germany) and mounted onto 400 mesh bare copper grids. Transmission electron microscopy was performed on a FEI Tecnai G2 transmission electron microscope run at 200 keV accelerating voltage and using a 20 µm objective aperture to improve contrast. Images were taken using an AMT camera at 5000-fold magnification.

***Quantification of mRNA transcripts using quantitative RT-PCR***. RNA was extracted from flash frozen A-type placentomes using QIAzol Lysis Reagent Solution and Qiagen miRNeasy purification columns (Qiagen, UK) according to manufacturer's specifications. RNA concentration was determined using a NanoDrop™ spectrophotometer. The ratio of absorbance between 260 nm/280 nm for all samples was over 2. RNA was reverse transcribed into cDNA using a RevertAid First Strand cDNA Synthesis Kit (Thermo Fisher, UK) according to manufacturer's specifications. qRT-PCR was performed using the SYBR® Green system (Thermo Fisher, UK) according to manufacturer's instructions in the 7500 Fast Real-Time PCR (Applied Biosystems). mRNA transcript levels of unknown genes were determined by the threshold cycle $\Delta\Delta C_t$ method and normalised to ribosomal protein L19 and glucose-6-phosphade dehydrogenase expression, which were not influenced by exposure to chronic long-term hypoxia. All primer sequences can be found in the Major Resources Table.

### *Plasma and urine analyses*

Plasma concentrations of soluble fms-like tyrosine kinase 1 (sFlt-1), soluble endoglin (sEng), placental growth factor (PlGF), vascular endothelial growth factor (VEGF) and creatinine and urine concentrations of albumin and creatinine were measured using commercially available colorimetric kits, according to manufacturer's instructions. A list of kits used can be found in the Major Resources Table. For sFlt-1, the inter- and intra-assay coefficients of variation were <12.0% and <10.0%, respectively, and the lower limit of detection was 0.1 ng/ml. For sEng, the inter- and intra-assay coefficients of variation were <15.0% for both, and the lower limit of detection was 0.1 ng/ml. For PlGF, the inter- and intra-assay coefficients of variation were <10.0% for both, and the lower limit of detection was 1.0 pg/ml. For VEGF, the inter- and intra-assay coefficients of variation were <15.0% and <10.0%, respectively, and the lower limit of detection was 1.0 pg/ml units. For creatinine, the inter- and intra-assay coefficients of variation were < 5.0% for both, and the lower limit of detection was 2.0 µg/ml. For albumin, the inter- and intra-assay coefficients of variation were <5.0% and <3.0%, respectively, and the lower limit of detection was 2 µg/ml. Measurements from plasma samples taken on 103 and 105 dGA before the onset of chronic normoxia or hypoxia were averaged as baseline measurements.

### *Longitudinal maternal arterial blood pressure and uterine vascular resistance*

A second cohort of pregnant ewes were surgically prepared with catheters and flow probes to permit continuous monitoring of arterial blood pressure and uterine blood flow in N and H groups via the CamDAS wireless data acquisition system [3-5]. In this second cohort, recording during chronic normoxia or chronic hypoxia occurred for 10 days, from 125 to 135 dGA.

***Surgery.*** The second cohort of pregnant Welsh mountain ewes carrying singleton fetuses underwent laparotomy at 116 ± 1 dGA for instrumentation with the wireless data acquisition system under general anesthesia, as previously described [3-5]. Animals were fasted for 24h prior to surgery with ad libitum access to water. On the day of surgery, animals were induced using Alfaxan (1.5-2.5 mg/kg alfaxalone, intravenously; Jurox Ltd., UK) into the jugular vein and then intubated (Portex cuffed endotracheal tube; Smiths Medical International Ltd., UK) using a laryngoscope for maintenance under general anesthesia using 1.5-2.0% isofluorane (IsoFlo; Abbott Laboratories Ltd., UK) in 60:40 oxygen:nitrogen using a positive pressure ventilator (Datex-Ohmeda Ltd., UK). Following induction, the maternal abdomen, flanks and medial surfaces of the hind limbs were shaved and cleaned, and an antibiotic (30 mg/kg procaine benzylpenicillin intramuscularly.; Depocillin; Intervet UK Ltd., UK) and an analgesic (1.4 mg/kg carprofen subcutaneously.; Rimadyl; Pfizer Ltd., UK) were administered. The ewe was then transferred to the surgery theatre and general anesthesia was maintained, as before. The animal was covered with sterile drapes and a midline abdominal incision was made, as described previously [7,8]. A Transonic flow probe (MC2RS-JSF-WC120-CS12-GCP, Transonics, UK) was positioned around the maternal uterine artery, as before, and then exteriorised through a keyhole incision in the ewe's right flank for connection to the wireless data acquisition system [3-5]. Following closure of the abdominal cavity, catheters were inserted via the maternal femoral vein (inner diameter 0.86 mm, outer diameter 1.52 mm; Critchly Electrical Products, Australia) into the maternal inferior vena cava, and via the maternal femoral artery (inner diameter 1.00 mm, outer diameter 1.60 mm; Altec, UK) into the maternal descending aorta. Catheters were exteriorised through a keyhole incision in the maternal left flank and connected to the wireless data acquisition system. While under general anesthesia, the ewe was then fitted with a bespoke jacket housing the wireless data acquisition system. After the end of anaesthesia, the ewe continued to be ventilated until spontaneous respiratory movements were observed, after which the ewe was extubated.

***CamDAS$^{TM}$ System.*** The wireless data acquisition system has been previously described in detail [3,4]. In brief, the CamDASTM (Maastricht Instruments, the Netherlands) consisted of a pressure box attached to one side of the ewe containing pressure transducers (COBE; Argon Division, Maccim Medical, USA) connected to catheters, and a miniaturised flow module on the other side connected to Transonic flow probes (Figure 1B in main text). The pressure and flow boxes were powered by Lithium batteries housed within the same jacket, allowing continuous wireless transmission and recording of maternal uterine blood flow and maternal arterial blood pressure beat-by-beat onto a laptop computer via Bluetooth technology. The weight of the CamDASTM system is less than 2 kg, thereby equivalent to the ewe carrying twins.

***Post-surgical recovery.*** Ewes were allowed to recover in a floor pen adjacent to other sheep with free access to hay and water and a 12:12 h light-dark cycle. Ewes were fed concentrates once a day (200g sheep nuts no. 6; H & C Beart Ltd., UK). Antibiotic (30 mg/kg procaine benzylpenicillin intramuscularly; Depocillin; Intervet UK Ltd., UK) and analgesic (1.4mg/kg carprofen subcutaneously; Rimadyl; Pfizer Ltd., UK) agents were administered to the ewe for five days following surgery. From 120 dGA ewes were fed the daily maintenance diet (5g hay/kg and 40g sheep nuts/kg; Manor Farm

Feeds Ltd., Oakham, UK) and pregnancies were randomly assigned to chronic normoxia (N) or chronic hypoxia (H) groups, as before.

***Chronic hypoxia, CamDAS recording and blood sampling.*** Following 3 days of post-surgical recovery, H ewes were transferred to the hypoxic chambers to acclimatise under normoxic conditions. Five days after surgery, at 125 dGA, H ewes were gradually subjected to hypoxia, reaching 10 ± 1 % inspired oxygen over 24 h, as before. Exposure to chronic hypoxia in this second cohort of surgically prepared H ewes lasted 10 days, until 135 dGA. In both N and H ewes, arterial blood samples were taken daily to measure maternal blood gases, acid-base excess and metabolic status, as previously described[7]. Continuous CamDAS$^{TM}$ recordings of maternal arterial blood pressure and uterine blood flow were converted into minute averages off-line. Uterine vascular resistance was calculated following Ohm's principle by dividing maternal arterial blood pressure by uterine blood flow [5]. Blood gas and acid base values were measured using an ABL5 blood gas analyser (Radiometer; Copenhagen, Denmark; maternal measurements corrected to 38$^{o}$C). Values for arterial oxygen saturation (Sat Hb) and haemoglobin (Hb) were determined using a haemoximeter (OSM3; Radiometer). Blood glucose and lactate concentrations were measured using an automated analyser (Yellow Springs 2300 Stat Plus Glucose/Lactate Analyser; YSI Ltd., Farnborough, UK). Values for Hct were obtained in duplicate using a microhaematocrit centrifuge (Hawksley, UK). Measurements from blood samples taken between 120 and 124 dGA before the onset of chronic normoxia or hypoxia were averaged as baseline measurements. At the end of *in vivo* experiments, N and H ewes were transported to the post-mortem laboratory and humanely killed as before. The position of the uterine Transonic flow probe and maternal catheter tips was verified.

### *Statistical analysis*

Appropriate power calculations derived from previous data sets were performed to determine the minimum sample size required to achieve statistical significance. Animals exposed to treatment were randomly chosen. Scientists measuring *ex vivo* outcomes were blinded to treatments. All data are expressed as mean ± SEM. The effect of treatment was analysed using the Student's *t* test for unpaired data. The effects of treatment, time and interactions between treatment and time were compared by two-way multiple comparison ANOVA. For all comparisons, values of $P < 0.05$ were accepted as statistically significant. The software used was Graphpad Prism 7 (RRID:SCR_002798).

## Supplemental References


1. Kilkenny C, Browne WJ, Cuthill IC, Emerson M, et al. Improving Bioscience Research Reporting: The ARRIVE Guidelines for Reporting Animal Research. PLoS Biology. 2010;8:e1000412. doi: 10.1371/journal.pbio.1000412

2. Brain KL, Allison BJ, Niu Y, Cross CM*, et al.* Induction of controlled hypoxic pregnancy in large mammalian species. *Physiological Reports*. 2015;3:e12614. doi: doi:10.14814/phy2.12614

3. Allison BJ, Brain KL, Niu Y, Kane AD*, et al.* Fetal in vivo continuous cardiovascular function during chronic hypoxia. *The Journal of Physiology*. 2016;594:1247-1264. doi: 10.1113/JP271091

4. Shaw CJ, Allison BJ, Itani N, Botting KJ*, et al.* Altered autonomic control of heart rate variability in the chronically hypoxic fetus. *The Journal of Physiology*. 2018;596:6105-6119. doi: 10.1113/jp275659

5. Jellyman JK, Gardner DS, Fowden AL, Giussani DA. Effects of dexamethasone on the uterine and umbilical vascular beds during basal and hypoxemic conditions in sheep. *American journal of obstetrics and gynecology*. 2004;190:825-835. doi: 10.1016/j.ajog.2003.09.046

## Supplementary Tables

| | N | | H | |
|---|---|---|---|---|
| | baseline | 135 dGA | baseline | 135 dGA |
| $PaO_2$ (mmHg) | 104.2 ± 1.9 | 98.0 ± 5.0 | 105.7 ± 3.7 | 42.0 ± 1.2 *† |
| $PaCO_2$ (mmHg) | 32.3 ±1.3 | 30.5 ± 2.5 | 33.6 ± 1.4 | 32.0± 1.5 |
| Sat Hb (%) | 102.6 ± 1.3 | 101.6 ± 3.5 | 103.5 ± 0.9 | 79.5 ± 6.1*† |
| Haematocrit (%) | 28.6 ± 1.1 | 28.5 ± 0.9 | 30.0 ± 1.2 | 33.9 ± 1.0 *† |
| Haemoglobin (g/dL) | 9.41 ± 042 | 9.20 ± 0.30 | 10.15 ± 0.08 | 11.23 ± 0.17 *† |
| pH | 7.49 ± 0.03 | 7.46 ± 0.06 | 7.50 ± 0.01 | 7.48 ± 0.01 |
| Glucose (mmol/L) | 2.60 ± 0.14 | 2.21 ± 0.03 | 2.78 ± 0.20 | 2.49 ± 0.22 |
| Lactate (mmol/L) | 0.56 ± 0.11 | 0.51 ± 0.06 | 0.61 ± 0.11 | 0.58 ± 0.06 |

***Table S1.*** *Maternal arterial blood gas, acid base and metabolic status.*
*Values are mean ± SEM for maternal arterial blood gas and, acid base and metabolic status at baseline and at 135 dGA. Groups are N (n=5) and H (n=5). Significant differences (P<0.05) are *N vs. H, or † vs baseline; two-way RM ANOVA.*

## Supplementary Figures

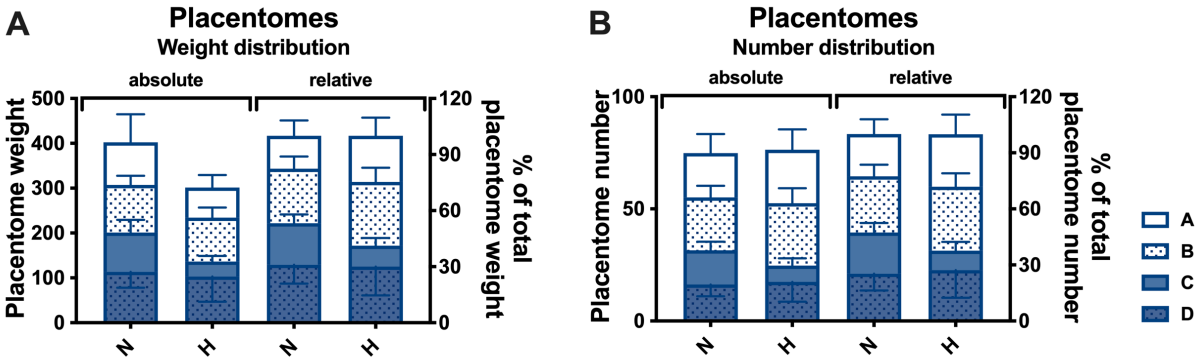


***Figure S1. Hypoxic pregnancy does not alter placentome distribution.*** *Values are mean ± SEM for the absolute and relative weight (A) and number (B) of A-, B-, C- and D-type placentomes. Groups are N (n=8) and H (n=6). There were no significant differences within or between groups.*

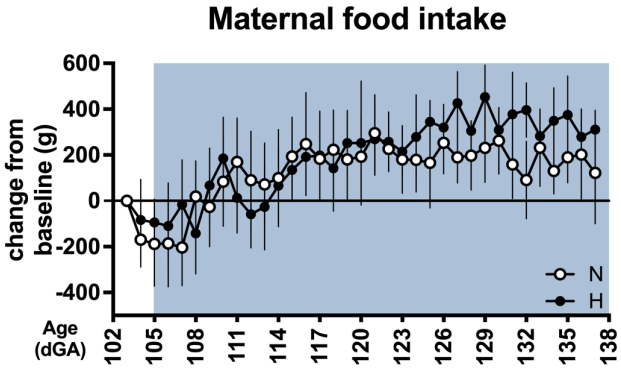


***Figure S2. Hypoxic pregnancy does not alter maternal food intake.*** *Values are mean ± SEM for the change in maternal food intake compared to baseline. Groups are N (○, n=9) and H (●, n=7). There were no significant differences within or between groups.*

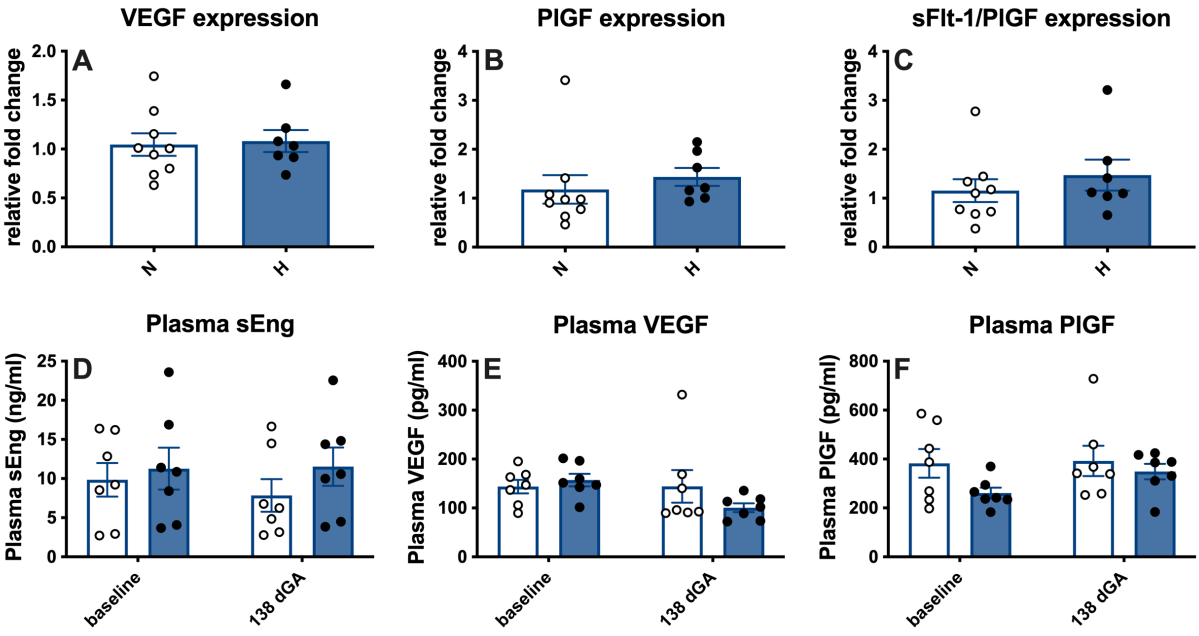


***Figure S3. Effects of hypoxic pregnancy on placental gene expression and maternal plasma concentrations of angiogenic factors.*** *Upper panel: Values are mean ± SEM for the relative fold change for VEGF (A), PlGF (B) and the ratio of sFlt-1 to PlGF (C) in placentomes at 138 dGA as measured by qRT-PCR. Lower panel: Values are mean ± SEM for the maternal plasma concentration of sEng (D), VEGF (E) and PlGF (F) at baseline and at 138 dGA as measured by ELISA. Groups are N (○, n=7-9) and H (●, n=7).*

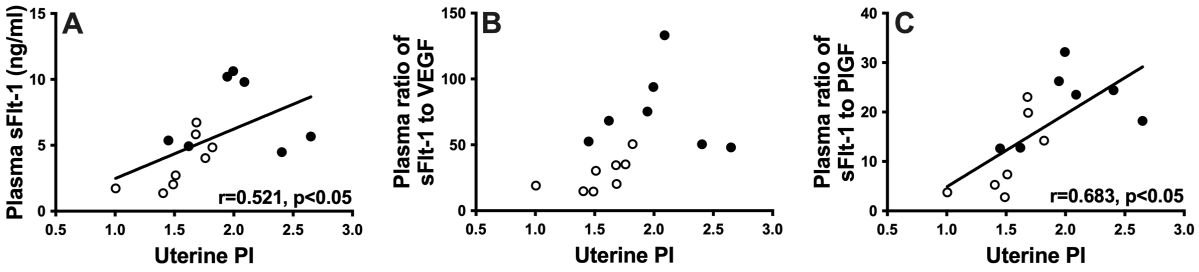


***Figure S4. Maternal angiogenic imbalance correlates with uteroplacental vascular resistance.*** *Correlation of maternal uterine artery PI with the plasma concentration of sFlt-1 (A), with the plasma ratio of sFlt-1 compared to VEGF (B) and with the plasma ratio of sFlt-1 compared to PlGF (C) at 138 dGA. Groups are N (○, n=7-8) and H (●, n=7). Significant correlation (P<0.05) determined by Pearson's correlation.*

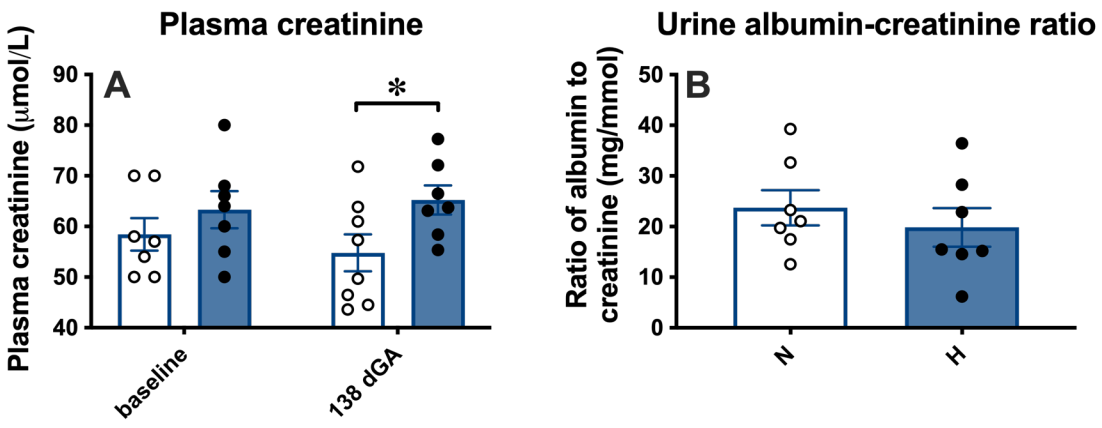


***Figure S5. Maternal renal function.*** *Values are mean ± SEM for the plasma concentration of creatinine during baseline and at 138 dGA (A) and the ratio of albumin to creatinine concentration in maternal urine at 138 dGA (B). Groups are N (○, n=7) and H (●, n=7).*